論文 / 著書情報
Article / Book Information

論題(和文)	主筋座屈に着目したRC 造梁の静的載荷実験 (その3)主筋座屈発生部材角の解析的評価
Title(English)	Static loading experiment of RC beams focusing on buckling of longitudinal bars Part 3 Analytical evaluation for drift at buckling of beam longitudinal bar
著者(和文)	PRADHAN SUJAN, 河村英里子, 尹ロク現, 真田 靖士
Authors(English)	PRADHAN Sujan, KAWAMURA Eriko, YOON Rokhyun, SANADA Yasushi
出典(和文)	日本建築学会大会学術講演梗概集, , , pp. 489-490
Citation(English)	, , , pp. 489-490
発行日 / Pub. date	2019, 9
権利情報	一般社団法人 日本建築学会

日本建築学会大会学術講演梗概集
（北陸） 2019 年 9 月

Static loading experiment of RC beams focusing on buckling of longitudinal bars
Part 3 Analytical evaluation for drift at buckling of beam longitudinal bar

Full scale test　Performance based design　Reinforced concrete　Safety limit　Seismic assessment

Member ○PRADHAN Sujan *1　Member KAWAMURA Eriko *1
Member YOON Rokhyun *2　Member SANADA Yasushi *3

1. Introduction

The details of experimental results on three full scale beam specimens were explained in **Part 2** [1]. This part describes an analytical evaluation for the drift at longitudinal reinforcing bar buckling of a prototype RC beam specimen (**Specimen 1**).

2. Evaluation for the Buckling of Longitudinal Bar

This section explains the evaluation method for the buckling of beam longitudinal reinforcing bar based on the previous evaluation method [2]. The details of the evaluation method are explained in the following sections.

2.1 Evaluation of the buckling resistance stress

As explained in **Part 2**[1], the buckling of beam longitudinal reinforcing bar was confirmed within two subsequent shear reinforcing bars at the beam end. Hence, the beam longitudinal reinforcing bars and the shear reinforcing bars were replaced with a line model to estimate the buckling occurrence limit point for longitudinal reinforcing bars. **Fig. 1** shows a conceptual diagram of beam longitudinal bar buckling. The existence of shear reinforcing bars were represented by fixed supports for the estimation of buckling occurrence limit point. Thus, the buckling resistance stress (σ_E) was evaluated by using **Eq. (1)**.

$$\sigma_E = \frac{4\pi^2 \cdot I}{L_B^2 \cdot A_r} \cdot E \tag{1}$$

where, I and A_r are the moment of inertia and the cross-sectional area of beam longitudinal reinforcing bar; L_B is the center to center distance of shear reinforcing bars (200 mm for **Specimen 1**) and E is the rigidity coefficient of the beam longitudinal reinforcing bar.

Since the values, except the rigidity coefficient E on the right side of the **Eq. (1)** can be determined from the beam properties, the buckling resistance strength (σ_E) is regarded as a function of the rigidity coefficient E. It is considered that the tensile yielding occurs before the occurrence of longitudinal reinforcing bar buckling and the rigidity reduces after the yielding of the longitudinal reinforcing bar. Hence, the rigidity coefficient E on the right side of **Eq. (1)** was replaced by the reduced (softened) modulus E_r.

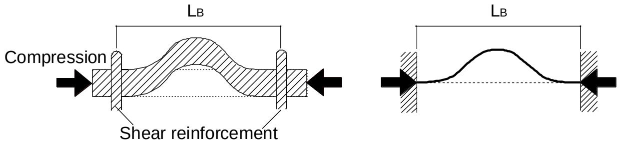

(a) Observation　　(b) Line model

Fig. 1 Conceptual figures of reinforcing bar reinforcement

2.2 Evaluation of reduced modulus E_r.

The reduced modulus E_r is the rigidity against bending deformation of the reinforcing bar after its yielding. In this study, the reduced modulus E_r was evaluated based on the method proposed by the previous researchers [2,3], which is briefly explained in this section. **Fig. 2** shows conceptual figures on the definition of reduced modulus E_r. When buckling of a beam longitudinal reinforcing bar occurs, the bending deformation creates regions where the strain increases and decreases in the cross-section of the longitudinal reinforcing bar. The rigidity coefficient becomes tangent rigidity E_h in the region where the strain increases, whereas that becomes elastic modulus E in the region where the strain decreases. Hence, the stress increment in reinforcing bar cross section occurs, as shown in **Fig. 2**. The neutral axis position θ_o in reinforcing bar cross section can be obtained from **Eq. (2)**, resulting from the balanced stress increments in the cross section. The value of tangent rigidity E_h can be obtained by determining the instantaneous rigidity on the investigated unloading stress-strain curve of longitudinal reinforcing bar. In this study, the modified Menegotto Pinto equation [4] was adopted, as given in **Eq. (3)**. The reduced modulus E_r can be obtained by substituting the evaluated values as explained above into the **Eqs. (4)** and **(5)**.

Hence, the buckling resistance strength (σ_E) was evaluated by using the **Eq. (1)**.

$$\frac{E_h}{E_s} = \frac{\left(sin\theta_0 - \frac{1}{3}sin^3\theta_0 - \theta_0 cos\theta_0\right)}{\left(sin\theta_0 - \frac{1}{3}sin^3\theta_0 + (\pi - \theta_0)cos\theta_0\right)} \tag{2}$$

$$\sigma_0 = 2\sigma_Y\left(H\frac{-\varepsilon_i}{2\varepsilon_Y} + \frac{(1-H)\frac{-\varepsilon_i}{2\varepsilon_Y}}{\left(1+\left|\frac{-3\varepsilon_i}{23_Y}\right|^R\right)^{1/R}}\right) + \sigma_i \tag{3}$$

$$\Phi(\theta) = \frac{1}{4}\left[\theta - \left(\frac{5}{2} - \frac{1}{3}sin^2\theta\right)sin2\theta + 4\theta cos^2\theta\right] \tag{4}$$

$$E_r = \frac{4E_s}{\pi}\left[\Phi(\theta_0) + \Phi(\pi - \theta_0)\frac{E_h}{E_s}\right] \tag{5}$$

In **Eq. (3)**

R is maximum excursion into plastic hinge and given by **Eq. (6)**.

$$R = R_0 - \frac{a_1\varepsilon_{max}}{a_2 + \varepsilon_{max}} \tag{6}$$

R_0 is the value of the parameter R at the first loading curve and a_1, a_2 are the parameters to be defined together with R_0

For the analysis, the values of the constants were taken from the past research [4], as: $H = 0.001$, $R_0 = 20.0$, $a_1 = 18.5$, $a_2 = 0.00015$.

2.3 Evaluation method of the rotation angle at buckling of longitudinal reinforcing bar

Fig. 3 shows the stress-strain relationship of the modified Menegotto-Pinto model and the Euler's buckling resistance strength curve obtained by substituting the reduced modulus E_r of each strain in the unloading curve of the modified Menegotto-Pinto model [4]. The reinforcing bar yields in tension and the tensile strain increases to the maximum tensile point (point A in **Fig. 3**); thus unloading starts. The buckling of the longitudinal reinforcing bars occurs at the point where the unloading curve and the buckling strength curve intersects (point B in **Fig. 3**), as beyond this point the buckling resistance strength (σ_E) becomes smaller than the working stress. In the proposing method, the compressive stress (σ_o) was assumed to reach zero under

主筋座屈に着目した RC 造梁の静的載荷実験
(その 3) 主筋座屈発生部材角の解析的評価

Pradhan Sujan，河村英里子，尹ロク現，真田靖士

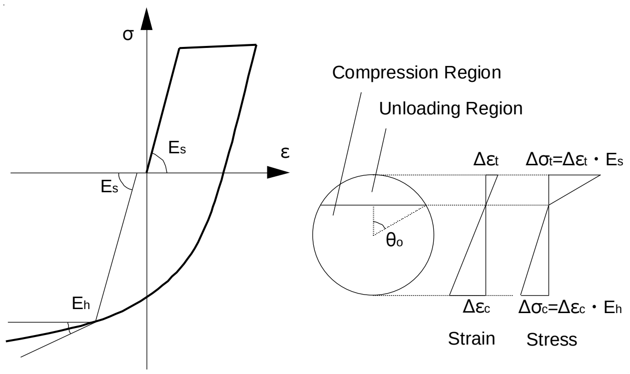

Fig. 2 Equivalent stiffness modulus

compression because the neutral axis was likely to close to the reinforcing bar position on the compressive side; namely, the intersection of both curves was assumed to be at point C in **Fig. 3**. Thus, the buckling limit strain (ε_B) can be evaluated, which is the strain at point A in **Fig. 3**.

The rotation angle at the buckling of longitudinal reinforcing bar (θ_B) was evaluated by using **Eq. 7**. Furthermore, it was assumed that the curvature was constant within the plastic zone.

$$\theta_{B(hinging)} = \frac{\varepsilon_B}{j_t} \cdot l_p \qquad (7)$$

where, j_t is the center to center distance of longitudinal reinforcing bars (= 569 mm) and l_p is assumed plastic hinge length (=350 mm) based on the experimental result, which is explained in detail in **Part 4**.

The analytical rotation angle at buckling of longitudinal reinforcing bar was found 1.26% rad based on the above procedure.

3 Verification of the Proposed Evaluation Method

This section verifies the evaluation method for the buckling of beam longitudinal reinforcing bar by comparing the rotation angle at buckling obtained from the analysis and the experiment. The rotation angle $({}_{test}\theta_B)$ at buckling of beam longitudinal bar from the experiment was evaluated as illustrated in **Fig. 5**. During the static loading experiment, the longitudinal reinforcing bars were pulled out from the stub, which affected the experimentally measured rotation angle. Hence, the experimentally measured rotation angle was corrected excluding the pullout effect to compare with the analytical rotation angle at buckling of longitudinal reinforcing bar. The pullout length was evaluated based on strains along the longitudinal reinforcing bar monitored by strain gauges [5]. The strain distribution between the two strain measured points were assumed to be linear, as shown in **Fig. 4**. **Table 1** compares the rotation angle at buckling of longitudinal reinforcing bar from the analysis and from the experiment.

The rotation angle from the analysis ($\theta_{B(hinging)}$= 1.26% rad) had a good agreement with that from the modified experimental buckling drift range (${}_{test}\theta_B$ -${}_{test}\theta_{B(Pullout)}$=0.92 to 1.30 % rad). Hence, the evaluation method as explained above is applicable to evaluate the rotation angle at buckling of beam longitudinal reinforcing bar.

4. Conclusion

The drift at buckling of beam longitudinal reinforcing bar was analytically evaluated. The evaluated drift at buckling of beam longitudinal reinforcing bar had a good agreement with that from the experiment.

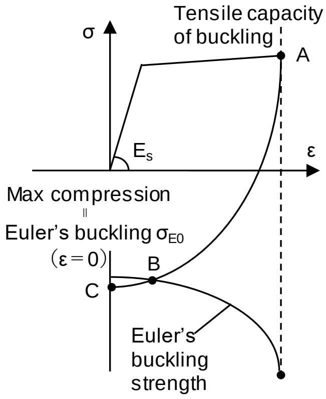

Fig. 3 Assumption of the calculation method

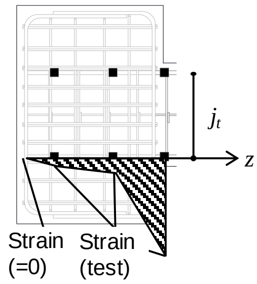

$${}_{test}\theta_{B(pullout)} = \frac{\int \varepsilon dz}{j_l}$$

at buckling

Fig. 4 Strain distribution in stub

$${}_{test}\theta_B = \left| \frac{(\delta_{1n} + \delta_{2n}) - (\delta_{1s} + \delta_{2s})}{j} \right|$$

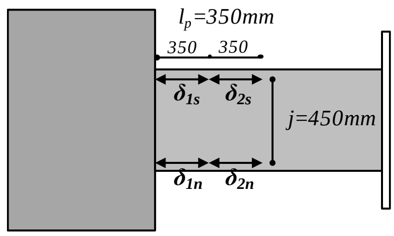

Fig. 5 Evaluation of rotation angle ${}_{test}\theta_B$ from experiment

Table 1 Ultimate drift angle of buckling

Ultimate strain at buck. ε_B	Rotation angle with hinging $\theta_{B(hinging)}$	Test	
		${}_{test}\theta_B$ -${}_{test}\theta_{B(Pullout)}$	Rotation angle with pullout ${}_{test}\theta_{B(Pullout)}$
0.0204	1.26	0.92 ~ 1.30	0.647 (R=1.62%rad)
			0.732 (R=2.18%rad)

Unit: %rad

[References]

[1] Kawamura, E., et al., Static Loading Experiment of RC Beams Focusing on Buckling of Longitudinal bars: Part2 Experimental Results and Discussions, Summaries of Technical Papers of Annual Meeting Architectural Institute of Japan, Structures Ⅳ, 245-246, 2018.

[2] Akiyama, M., Naito, H. and Suzuki, M.: Calculation Method of Ultimate Curvature of RC and SRC Section Based on Analytical Model for Axial Reinforcement Buckling and Its Application to Ductility Evaluation of These Columns., Journal of JSCE,58(725), 113-129, 2003. (in Japanese).

[3] Papis, M., Russo, G. and Zingone, G.: Instability of Longitudinal Bars in RC Columns., Journal of Structural Engineering, 114(2), 445-461.1988.

[4] Naganuma, K., Ohkubom, M.: An Analytical Model for Reinforced Concrete Panels Cyclic Stresses, Journal of Structural and Construction Engineering (Transactions of AIJ), Vol.65, No.536, pp.135-142, 2000.10 (in Japanese).

[5] Architectural Institute of Japan: Design Guidelines for Earthquake Resistant Reinforced Concrete Buildings Based on Inelastic Displacement Concept (Draft). 1997 (in Japanese).

*1 Graduate Student, Graduate School of Eng., Osaka Univ.
*2 Asst. Prof., Graduate School of Eng., Osaka Univ., Dr. Eng.
*3 Prof., Graduate School of Eng., Osaka Univ., Dr. Eng.

*1 大阪大学大学院工学研究科　大学院生
*2 大阪大学大学院工学研究科　助教　博士(工学)
*3 大阪大学大学院工学研究科　教授　博士(工学)